Original Research

The Applicability of a Human Immunohistochemical Panel to Mouse Models of Hepatocellular Neoplasia

Kenneth J Salleng,[1,*] Frank L Revetta,[2] Natasha G Deane,[3] and M Kay Washington[2]

Various immunohistochemical panels are used as aids to distinguish between primary hepatocellular malignancies and metastatic tumors and between benign lesions and carcinomas. We compared the immunohistochemical spectrum of hepatocellular lesions in mice with that of human hepatocellular carcinoma (HCC). Specifically, we compared the staining parameters of 128 murine foci of cellular alteration (FCA) and tumors (adenoma and HCC) from archival tissue blocks of 3 transgenic mouse models (LFABP–cyclin D1, Alb1–TGFβ1, and LFABP–cyclin D1 × Alb1–TGFβ1) with those of archival human HCC ($n = 5$). Antibodies were chosen according to their published performance and characterization in human hepatocellular tumor diagnosis and included: arginase 1 (Arg1), β-catenin, glutamine synthetase (GS), glypican 3, hepatocyte paraffin 1 (HepPar1), and cytokeratin 19 (CK19). GS was the single best immunostain for identifying hepatocellular tumors in mice, with 100% positive staining. Data showed a trend toward loss of normal function (staining) with Arg1, with a higher percentage of positive staining in FCA than in adenomas and HCC. All FCA lacked murine β-catenin nuclear translocation, which was present in 2 of the 7 adenomas and 22 of the 96 HCC tested. HepPar1 staining was lower than anticipated, except in trabecular HCC (16 of 22 samples were positive). Glyp3 stained very lightly, and only scattered CK19-positive cells were noted (4 of 44 cases of mouse trabecular HCC). Thus, GS appears to be the most useful marker for identifying neoplasia in the transgenic mouse models we tested and should be included in immunohistochemistry assessing hepatocellular neoplasia development.

Abbreviations: Arg1, arginase 1; CK19, cytokeratin 19; FCA, foci of cellular alterations; GS, glutamine synthetase; Glyp3, glypican 3; HepPar1, hepatocyte paraffin 1; HCC, hepatocellular carcinoma; HSP70, heat-shock protein 70; LFABP, liver fatty acid binding protein; pCEA, polyclonal carcinoembryonic antigen.

Neoplasia remains one of the major causes of human morbidity and mortality on a global scale. In the United States alone, 1 of every 4 deaths can be attributed to cancer.[46] Worldwide, primary liver cancer is the fifth most common type of cancer diagnosed and the third most common cause of cancer related death.[5,24] Hepatocellular carcinoma (HCC) represents the single most commonly diagnosed form of primary liver cancer.[14] Given the rising rates of hepatocellular cancer both within the United States and globally, in 2012 the NIH provided $73 million in funding specifically for liver cancer research studies.[40] Research utilizing animal models of carcinogenesis is imperative for understanding the development and progression of cancer, as well as aid in the formulation of therapies. Transgenic mouse models often mimic human disease. The mouse lines Tg(Fabp1–Ccnd1)4Rdb, Tg(Alb1–TGFβ1)1Sst, and Tg(Alb1–TGFβ1)1Sst × Tg(Fabp1–Ccnd1)4Rdb have all been shown to develop multiple spontaneous hepatocellular neoplasms (adenomas and HCC) along with foci of cellular alteration (FCA) within the same animal.[10,11] Hepatocellular changes in rodents range from FCA to adenomas and HCC. FCA have been considered preneoplastic lesions in rodents and do not have a well-defined human counterpart. In addition, the FCA are phenotypically different from adjacent normal hepatocytes, which fuels the concern that they are preneoplastic lesions.[34]

The aforementioned transgenic models develop hepatocellular changes through different mechanisms. Tg(Fabp1–Ccnd1)4Rdb mice (LFABP–cyclin D1 mice) use a liver fatty acid binding protein (LFABP) promoter to overexpress cyclin D1, which regulates the progression of the cell cycle. LFABP specifically targets overexpression of cyclin D1 to the liver, causing the development of progressive neoplastic lesions (including HCC) in that tissue.[10,11] Tg(Alb1–TGFβ1)1Sst mice (Alb1–TGFβ1 mice) have a modified TGFβ cDNA that is controlled by the regulatory portion of the albumin gene. TGFβ governs the inhibition of hepatocellular growth after hepatic injury and regulates apoptosis and the development of fibrosis.[45] LFABP1–cyclin D1 × Alb1–TGFβ1 mice (Tg[Alb1–TGFβ1]1Sst × Tg[Fabp1–Ccnd1]4Rdb) overexpress cyclin D1, which overrides the tumor-suppressing abilities of TGFβ but maintains some of the tumor-promoting effects of TGFβ.[10]

Many approaches exist in diagnosing hepatocellular neoplasms, but the standard remains the histologic evaluation of tissue. Immunohistochemistry is used to help define the characteristics of hepatocellular tumors and provide insight into determining adenomas from HCC. No single marker has been found that is completely specific for HCC, so various panels have been developed as diagnostic aids. Data regarding the relative immunohistochemical staining characteristics of murine FCA, adenomas, and HCC (along with their comparison to Human HCC) are sparse, even though these animals are used as models in studying cancer development. To characterize the comparative immunostaining characteristics of the hepatocellular tumors of mice and humans, we selected a panel of antibodies in light of their specificity for hepatocellular neoplasia in human samples and their well-described and published performance profile. We evaluated immunohistochemical markers: arginase 1 (Arg1), β-catenin, glutamine synthetase (GS), glypican 3 (Glyp3), hepatocyte paraffin 1 (HepPar1), and cytokeratin 19 (CK19). Of these, Arg1 and HepPar1 are expressed in normal human hepatocytes and are consequently particularly useful in defining neoplasms of hepatic origin.[4,38,41,52,60] The Arg 1 metalloenzyme is present in the urea cycle and is responsible for converting arginine into urea and ornithine. This protein is expressed in normal liver with diffuse cytoplasmic or cytoplasmic and nuclear expression[60] and may have either diffuse or focal expression in HCC.[52] The HepPar1 antibody measures carbamoyl phosphate synthetase 1, found in the urea cycle of the mitochondria.[4,38] Granular cytoplasmic localization is evident and associated with mitochondrial expression.[38,56] This immunostain serves as a positive marker for liver cells and shows high sensitivity and specificity for both well-differentiated neoplastic and normal hepatocytes. Decreased sensitivity is noted in poorly differentiated human HCC.[8,41,56] The hepatocellular enzyme GS is associated with the metabolism of ammonia and is a noted downstream target of the Wnt signaling pathway. Zonal expression (zone 3 hepatocytes) of GS is high in normal liver and follows a pericentral hepatocellular pattern. Normal pericentral hepatocytes and neoplastically transformed cells display a homogeneous cytoplasmic pattern of staining.[16,30] Altered location and activity of GS is noted in neoplastic development.[19,20]

For β-catenin and Glyp3, which are not found in normal liver tissue, the overexpression of these proteins is indicative of neoplastic transformation.[47,58,59] β-catenin is a component of both the cellular adhesion complex and the Wnt signaling pathway, which controls zonal regulation of many genes within the adult liver. Rodent studies have shown that normal hepatocytes usually have membranous localization, whereas neoplastic hepatocytes (adenomas and HCC) show both membranous and cytoplasmic staining in an oxazepam-induced model.[30] Normal human liver may have a thin membranous outline of hepatocytes.[54] Once the degradation of β-catenin is instigated by stimulation of the Wnt signaling pathway, it translocates to the nucleus.[2] Nuclear translocation has been noted in rodent hepatic tumors.[6] The heparin sulfate proteoglycan Glyp3 binds to the outer surface of plasma membranes and regulates the signaling controlling the activity of various growth factors. Glyp3 expression has commonly been noted as cytoplasmic, membranous, and sometimes canicular.[38,59] Glyp3 typically is not present in normal adult human liver tissue but has been shown to be expressed in fetal liver and poorly differentiated HCC.[26,59,61] Cytokeratin 19 is an intermediate filament protein that is present in many epithelial cells. It shows strong cytoplasmic staining in cholangiolar cells and in normal liver is expressed in bile duct epithelium. Because the 2 major primary hepatic tumors are hepatocellular and cholangiocellular in origin and because CK19 is expressed in 85% to 100% of human cholangiocarcinomas, we included this marker to aid in the differentiation between HCC and cholangiocarcinoma.[1,37,44,58]

The aims of this retrospective study were 1) to evaluate and compare the utility of an immunohistochemistry panel in 3 murine models of hepatic carcinogenesis (LFABP–cyclin D1, Alb1–TGFβ1 and LFABP–cyclin-D1X Alb1–TGFβ1) with published reports of human HCC and 2) to determine whether the expression of the selected markers varies along the spectrum of neoplastic transformation, from FCA to adenomas to various subtypes of HCC .

Materials and Methods

Animals. Archived liver samples from 12- to 18-mo-old, male and female mice including 15 homozygous LFAPB–cyclin D1 transgenic mice, 6 littermate WT control animals, 5 double-transgenic LFABP–cyclin D1 × Alb1–TGFβ1 mice, and a single Alb1–TGFβ1 mouse were used for the study. C57BL/6 mice were used to establish the transgenic lines. All mice used in the study were maintained in accordance with the *Guide for the Care and Use of Laboratory Animals* at Vanderbilt University, an AAALAC-accredited institution, and all procedures were approved by the Vanderbilt University IACUC.

Transgenic mouse lines were raised inhouse, and any animal manipulations required used microisolation techniques. All mice in the study were housed in individually ventilated caging, maintained on CareFresh Bedding (Absorption Corporation, Jesup, GA), and food and water were provided free choice. Mice were fed a standard chow diet (Lab Diet 5001, PMI Nutrition International, St Louis, MO), and acidified water was supplied by an automatic watering system through lixit valves. The housing rooms were maintained on a 12:12-h light:dark cycle with ambient room temperatures of 72 °F (± 2 °F; 22.2 ± 1.1 °C). Soiled-bedding sentinels were used for health monitoring and tested quarterly for common murine pathogens including endoparasites, ectoparasites, ectromelia virus, epizootic diarrhea of infant mice virus, Theiler murine encephalitis virus, K virus (mouse pneumonitis virus), lymphocytic choriomeningitis virus, mouse adenovirus 1 and 2, mouse hepatitis virus, *Mycoplasma pulmonis*, minute virus of mice, and mouse parvovirus (although mouse parvovirus is endemic in the facility where the animals were housed). *Helicobacter* testing of the mice was not performed, given that these species are not excluded pathogens in this facility.

Human tissue collection. De-identified formalin-fixed paraffin-embedded HCC samples were chosen from 5 surgical resections from the surgical pathology archives; 4 of the 5 samples also contained adjacent nonneoplastic liver. All human tissue samples had been fixed in 10% neutral buffered formalin for at least 24 h prior to routine processing and paraffin-embedding.

Mouse tissue collection. For tissue collection and immunohistochemistry, sections from the left liver lobe of mice were harvested and placed in 4% paraformaldehyde for 4 to 8 h prior to processing. Some samples then were transferred to 70% ethanol prior to processing. Fixed tissues were then routinely processed by dehydration and embedded in paraffin. Sections (5 µm) were trimmed and placed on charged slides for staining with hematoxylin and eosin and the selected battery of immunohistochemical markers.

All unstained slides were deparaffinized prior to immunohistochemical staining. All incubations were done at room temperature. To block nonspecific staining when Arg1, β-catenin, and HepPar1 were used, samples were treated with Mouse Ig Blocking Reagent (Vector Labs, Burlington, CA) for 60 min followed by a 15-min incubation in Serum Free Block (Dako, Carpenteria, CA).

Immunohistochemistry. Information regarding antibodies and antigen retrieval is outlined in Figure 1. All sections underwent antigen retrieval, antibody dilution, incubation times, and nonspecific protein blocking as described in Figure 1, followed by detection (Envision + HRP Labeled Polymer, Dako) for 20 min and application of DAB chromagen with a 5-min incubation to visualize reaction products. Slides were allowed to cool to room temperature. Normal liver was used as positive and negative control tissue, was included in every immunohistochemistry run, and was evaluated as appropriate to the marker. Inherent internal liver staining was evaluated for each stain. For CK19 staining, all steps except dehydration, clearing, and coverslipping were done on an automated stainer (Bond Max, Leica, Buffalo Grove, IL). Briefly, slides were deparaffinized; heat-induced antigen retrieval was performed by using Epitope Retrieval 2 solution (Leica) for 10 min. Slides were incubated with antiCK19 (dilution, 1:100) for 1 h. The Bond Refine Polymer detection system (Leica) was used for visualization. Slides were then dehydrated, cleared, and coverslipped.

Histologic evaluation. Liver samples from mice were stained with hematoxylin and eosin and evaluated for histologic evidence of neoplasia. FCA, adenomas, and HCC subtypes were diagnosed according to published criteria.[12,35,51] FCA were identified by their tinctorial staining characteristics, typical round to oval shape, and lack of disruption of overall normal liver architecture. FCA that are commonly diagnosed in rodent livers include vacuolated, clear-cell, eosinophilic, and basophilic foci.[12,51] Adenomas were defined as circumscribed lesions composed of well-differentiated hepatocytes that compressed adjacent hepatocytes. Hepatic plates were 1 to 3 cell-layers thick, with an irregular pattern of growth and loss of normal lobular architecture (Figure 2 C). HCC were diagnosed as tumors in which marked cellular pleomorphism was evident, with abnormal lobular architecture, increased mitotic figures, and any evidence of infiltration or invasion. In addition, HCC were subclassified by growth patterns as adenoid, solid, or trabecular. Adenoid HCC were defined as those tumors showing clear spaces surrounded by one or more layers of neoplastic hepatocytes (Figure 2 D). Solid HCC were identified by pleomorphic, poorly differentiated hepatocytes, with increased mitoses, atypia, and lack of an identifiable growth pattern (Figure 2 E). Trabecular HCC were defined by the presence of distinct cords of hepatocytes varying in cellular thickness and separated by sinusoidal spaces (Figure 2 F).[23,51]

Murine sections showing no evidence of neoplastic changes were reported as normal. All antibody localization was evaluated according to location as cytoplasmic, membranous, or nuclear.

Human specimens were all diagnosed as HCC by a surgical pathologist (MKW) according to standard diagnostic criteria.[22] All immunostains were scored by a single reader (KJS).

Results

Hematoxylin- and eosin-stained sections of murine liver (n = 25) were screened for the presence of FCA, adenomas, and HCC (adenoid, solid, and trabecular variants). Sections containing lesions of interest were immunostained and evaluated. FCA were routinely circular or oval, and only vacuolated foci (Figure 2 A) and clear-cell foci (Figure 2 B) were identified in the sections examined; no eosinophilic, basophilic, or mixed foci were noted. FCA embedded within a distinct HCC tumor were categorized as a part of the representative HCC. The numbers of each FCA or tumor are listed in Table 1 according to transgenic mouse strain. Because multicentric development of hepatocellular neoplasia has been reported to occur in the mouse strains used, each tumor was counted separately[10,11]. In addition, individual sections of mouse liver in the current study often showed multiple types of tumors (adenoma and different HCC variants) andFCA.

In the 25 mice, a total of 108 FCA and tumors were identified (Table 1). WT mice (n = 6) showed no evidence of distinct neoplasia, although one sample included a single clear-cell focus. The Alb1–TGF β1 mouse had a single clear-cell focus and 2 tumors, whereas the 13 LFABP–cyclin D1 mice had an average of 5.7 FCA or tumors per mouse. The 5 LFABP–cyclin D1 × Alb1–TGF β1 mice had an average of 3.4 FCA or tumors per animal.

Vacuolated foci (n = 12) were seen in 3 mice. One lesion was found in the liver of each of 2 LFABP–cyclin D1 mice, and 10 distinct vacuolated lesions were found in the liver of a single LFABP–cyclin D1 × TGF β1 mouse. In addition, 13 clear cell foci were noted in 6 mice (1 WT, 1 Alb1–TGFβ1, and 4 LFABP–cyclin D1 mice). Adenomas (n = 7) were present in 7 different mice (1 Alb1–TGFβ1, 3 LFABP–cyclin D1, and 3 LFABP–cyclin D1 × Alb1–TGFβ1 mice).A total of 59 adenoid HCC were present in 2 LFABP–cyclin D1 mice. Nine mice had 15 solid HCC (1 Alb1–TGFβ1, 5 LFABP–cyclin D1, and 3 LFABP–cyclin D1 × Alb1–TGF β1 mice), whereas 22 trabecular HCC were identified in 10 mice (1 Alb1–TGFβ1, 6 LFABP–cyclin D1, and 3 LFABP–cyclin D1 × Alb1–TGFβ1 mice). The staining pattern of tumors of the same subtype often varied within the same animal.

For all FCA and tumors, overall immunostaining (with the exception of β-catenin) was counted as positive when 5% or more of the cells within a FCA or tumor showed expression. This set point was established based on a previously published scoring system useful with a majority of the antibodies.[32,38] For β-catenin, we chose a positive set point of 1% or more of the cells within the FCA or tumor cells with nuclear expression. A summary of the staining results is noted in Table 2.

Arg1. Cytoplasmic or nuclear immunoreactivity (or both) for Arg1 was noted in all WT mouse liver sections and in the transgenic mouse samples Arg1 staining intensity varied markedly (Figure 3 A through C). Although Arg1 stained FCA (77% to 92%) and adenomas (71%) more frequently than the HCC subtypes, in some cases, normal liver and FCA showed only nuclear or variable cytoplasmic staining (Figure 3 C). Of the adenoid, solid and trabecular HCC, only 37%, 47% and 45% showed positive staining, respectively. In the human tissue examined, 4 of the 5 HCC samples stained positively.

β-catenin. All normal mouse liver sections, including WT, had faint nonspecific staining along hepatic sinusoids. Bile ducts and neoplastic and nonneoplastic hepatocytes showed membranous expression. Nuclear expression (translocation) was never as prominent as either cytoplasmic or membranous staining. All FCA were negative for β-catenin nuclear expression, whereas positive nuclear staining was found in representatives of all tumor types. In particular, 2 of the 7 adenomas had nuclear translocation (Figure 3 D), whereas 22 of 96 HCC (all variants) showed some positivity. This total includes adenoid (1 of 59 samples), solid (7 of

	Vendor	Catalog no.	Species	Dilution	Antigen retrieval	Blocks and times
Arginase 1	Abcam (Cambridge, MA)	Ab117989	Mouse monoclonal	1:200	None	Mouse on Mouse Serum-Free Protein Block (Vector Labs, Burlingame, CA), 15 min
β–catenin	BD Biosciences (San Jose, CA)	610154	Mouse monoclonal	1:1000	Citrate buffer, pH 6.0, 104 °C	Mouse on Mouse Serum-Free Protein Block (Vector Labs, Burlingame, CA), 15 min; followed by Serum-Free Block (Dako, Carpenteria, CA), 15 min
Glutamine synthetase	Abcam (Cambridge, MA)	Ab 73593	Rabbit polyclonal	1:1000	Citrate buffer, pH 6.0, 100 °C	Serum-Free Block (Dako, Carpenteria, CA), 15 min
Glypican 3	Abcam (Cambridge, MA)	Ab66596	Rabbit polyclonal	1:50	Citrate buffer, pH 6.0, 100 °C	Serum-Free Block (Dako, Carpenteria, CA), 15 min
Hepatocyte paraffin 1	Dako (Carpinteria, CA)	M7158	Mouse monoclonal	1:200	Citrate buffer, pH 6.0, 97 °C	Mouse on Mouse Serum-Free Protein Block (Vector Labs, Burlingame, CA), 60 min; followed by Serum-Free Block (Dako, Carpenteria, CA), 15 min
Cytokeratin 19	Protein Tech/Acris (San Diego, CA)	14965-1-AP	Rabbit polyclonal	1:100	EDTA, pH 9.0, 100 °C	Not applicable

Figure 1. Antibodies and antigen retrieval systems used for immunohistochemistry in the current study.

15), and trabecular (14 of 22) HCC tumors. Among the 5 human samples, only 1 (20%) showed positive nuclear β-catenin activity (Figure 3 E). This figure is slightly less than the reported range of 25% to 32% positivity.[21,58]

GS. WT mouse liver sections and nontumorous areas from all liver sections (mouse and human) showed positive expression (cytoplasmic, membranous, and nuclear) of GS in zone 3 pericentral hepatocytes (Figure 4 A). All murine tumors were GS-positive (Figure 4 C through E), whereas FCA showed positivity in 77% of clear-cell foci and 92% of vacuolated foci. The tumors were so well stained and differentiated from adjacent liver that it was often easy to identify tumors within the liver without placing the slide under the microscope. GS-positive FCA and tumor cells showed cytoplasmic and membranous, but only rarely nuclear, immunoreactivity. Some clear-cell foci were adjacent to, or lying within, zone 3 (Figure 4 B). Whether the staining in the clear cell foci was due to location or to preneoplastic proliferation was difficult to assess. In addition, 2 of the 5 human tumors showed distinct immunoreactivity, and the remaining 3 samples showed scattered rare positive cells (Figure 4 F).

Glyp3. Glyp3-positive hepatoctyes showed faint membranous or cytoplasmic staining (or both) which made differentiation difficult in the mouse sections (Figure 3 F). Staining that was increased in intensity was routinely present in the biliary epithelium. One third (4 of 12) of the vacuolated foci were positive with a minimal amount of staining, whereas 62% of the clear-cell foci showed some staining. Overall more of the mouse tumors were positive than were the FCA, with positive staining in 86% of adenomas, 60% of solid HCC, 86% of trabecular HCC, and 90% of adenoid HCC. All human HCC sections showed lightly positive membranous or cytoplasmic staining (Figure 3 G).

HepPar1. Tumors and FCA in the mouse sections showed cytoplasmic immunostaining of scattered individual or small groups of hepatocytes with HepPar1. Nontumorous sections of mouse liver showed positive but inconsistent cytoplasmic immunoreactivity. Fewer FCA (23% to 25%) showed positive staining for HepPar1 when compared with the tumors (adenomas at 43% and HCC ranging from 40% to 73%). Figure 3 H shows HepPar1 staining of a murine trabecular HCC variant. Nontumorous liver from human sections showed positive granular cytoplasmic expression of HepPar1 in normal and neoplastic hepatocytes (Figure 3 I).

CK19. All liver sections showed intense cytoplasmic staining of biliary epithelium. With the exception of 4 trabecular HCC, all murine FCA and tumors were negative for CK19 immunostaining. The 4 CK19-positive trabecular HCC were present in LFABP–cyclin D1 (n = 3) and LFABP–cyclin D1× Alb1–TGF β1 (n = 1) mice. CK19 has been shown to be expressed in very low numbers in HCC, and when positive, it produces patchy staining (Figure 3 K). In these mouse liver sections, scattered cells, which were mostly in the center of the neoplasm, showed cytoplasmic and membranous staining. All human tumors were negative for CK19 staining (Figure 3 L). CK19 has been reported as a marker for progenitor cells in the liver, thus perhaps explaining the presence of CK19 in some HCC.[13,28]

Discussion

This proof-of-principle project shows that some immunomarkers used for the diagnosis of human HCC can be applied successfully to the evaluation of FCA and primary hepatocellular neoplasms in mouse models. Not every tumor will stain for all markers, and this variability in immunophenotype often complicates diagnosis. An understanding of each immunomarker's performance is essential for interpretation. Markers that are expressed in normal hepatocytes (Arg1, GS, and HepPar1), are expected to show loss of function or aberrant zonal expression in poorly differentiated HCC. Markers that are not typically present in normal liver may show upregulation (Glyp3) or nuclear translocation (β-catenin). Distinguishing the 2
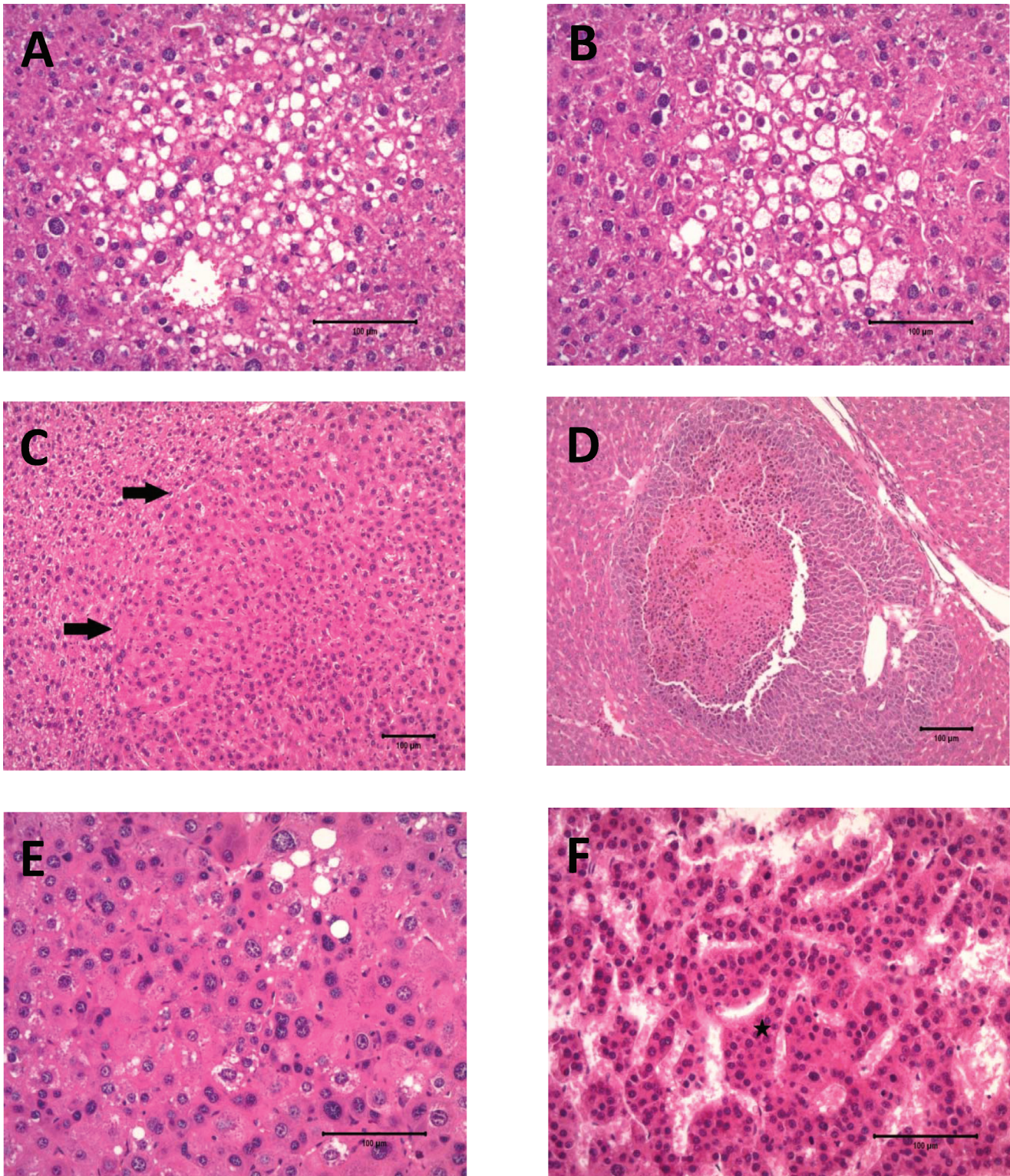
Figure 2. Murine Foci and HCC variants: hematoxylin and eosin stain. (A) Vacuolated foci; magnification, 20×. (B) Clear-cell foci; magnification, 20×. (C) Adenoma (arrows, margin); magnification, 20×. (D) Adenoid HCC; magnification, 10×. (E) Solid HCC variant; magnification, 20×. (F) Trabecular HCC variant showing thickening of hepatic plates (star); magnification, 20×.

primary hepatocellular tumors (HCC and cholangiocarcinoma) is essential, and histologic evaluation is often sufficient except in the case of poorly differentiated tumors. Histologic features of HCC can be seen in cholangiocarcinomas and include thickened hepatic cords resembling trabeculae or solid-tumor formation.[12] CK19, which stains cholangiocytes, can be used to help in this differentiation.

Table 1. Numbers of FCA, adenomas, and HCC variants

Mouse genotype	n	Vacuolated FCA		Clear-cell FCA		Adenoma		Adenoid HCC		Solid HCC		Trabecular HCC	
		No. foci	No. mice	No. foci	No. mice	No. sites	No. mice	No. sites	No. mice	No. sites	No. mice	No. sites	No. mice
WT (control)	6	0	0	1	1	0	0	0	0	0	0	0	0
ALB1-TGFβ1	1	0	0	1	1	1	1	0	0	1	1	2	1
LFABP–cyclin D1	13	2	2	11	4	3	2	59	2	10	5	7	6
LFABP cyclin D1 × Alb1–TGF β1	5	10	1	0	0	3	3	0	0	4	3	13	3
Total	25	12	3	13	6	7	7	59	2	15	9	22	10

Table 2. Summary of positive immunohistochemistry results from mouse and human liver samples

	Mouse FCA		Mouse adenoma	Mouse HCC			Human HCC	
	Vacuolated	Clear-cell		Adenoid	Solid	Trabecular	This study	Reported range
HepPar1	3/12 (25%)	3/13 (23%)	3/7 (43%)	34/59 (58%)	6/15 (40%)	16/22 (73%)	5/5 (100%)	26%[29] to 70%[42]
Glyp3	4/12 (33%)	8/13 (62%)	6/7 (86%)	56/59 (95%)	9/15 (60%)	19/22 (86%)	5/5 (100%)	40%[58] to 79%[29]
Arg1	11/12 (92%)	10/13 (77%)	5/7 (71%)	22/59 (37%)	7/15 (47%)	10/22 (45%)	4/5 (80%)	~85%[15,29,42]
GS	11/12 (92%)	10/13 (77%)	7/7 (100%)	59/59 (100%)	15/15 (100%)	22/22 (100%)	4/5 (80%)	54%[49] to 70%[33]
β-catenin	0/12 (0%)	0/13 (0%)	2/7 (29%)	1/59 (2%)	7/15 (47%)	14/22 (64%)	1/5 (20%)	25%[21] to 32%[58]
CK19	0/12 (0%)	0/13 (0%)	0/7 (0%)	0/59 (0%)	0/15 (0%)	4/22 (18%)	0/5 (0%)	10%[13] to 27%[57]

Murine Arg1 followed a similar staining pattern to reports in the human literature, with more FCA (77% to 92%) and adenomas (71%) expressing positivity than HCC (Table 2). The Arg1 positivity of mouse HCC staining ranged from 37% to 47%, whereas averages of 84.1% to 85% have been reported for human HCC.[15,29,38,42] Arg1 reactivity in human tumors decreases from 100% in well-differentiated HCC to 96.2% for moderately differentiated HCC and 85.7% for poorly differentiated HCC.[60] Arg1 is important for distinguishing the hepatocellular origin of tumors. In the mouse sections we evaluated, the overall Arg1 staining decreased with the progression from FCA to adenomas to HCC. Individual mice showed variation in Arg1 staining between tumors.

Immunomarkers associated with neoplastic transformation (for example, β-catenin and Glyp3) rather than cellular differentiation are more difficult to interpret in mice. A study evaluating hepatic neoplasia development in mice treated with oxazepam found that all neoplasms (n = 10) showed membranous and cytoplasmic localization of β-catenin, although no nuclear activation was identified.[30] Variability in nuclear β-catenin localization has been reported and depends on the underlying genetic mechanisms of the particular tumor. Nuclear translocation of β-catenin was identified in subsets of rodent hepatic tumors, including those in c-myc and c-myc–TGFβ1 transgenic mice.[6] Increased nuclear staining in tumors with β-catenin mutations in conjunction with increased proliferation rates (as indicated by increased Ki67 staining) has been noted in some neoplasms.[54] Activation of β-catenin is associated with the expression of other zonal genes, including GS.[9] In the current study, 2 of the 7 murine adenomas showed nuclear expression. This pattern might represent a well-differentiated HCC or a nuclear β-catenin–positive adenoma subtype, similar to that in the previously mentioned GS-coexpressing human tumors, or a

high risk for HCC development.[3,48] Both murine adenomas showing nuclear β-catenin translocation were GS-positive (data not shown). Given the variability of β-catenin as an immunomarker, its use in mice is of questionable benefit, and its value would depend on the molecular features of the model being studied.

Hepatocellular neoplasms diffusely express GS, without limitation to the normal pericentral (zone 3) expression.[20] Normal GS-positive cells other than pericentral hepatocytes include: cholangiocytes, endothelial cells and macrophages. In mice, hepatocellular adenomas express differing levels of GS depending on the type of mutation within the neoplasm. For example, Ha-ras–mutated lesions have almost undetectable GS levels, whereas Catnb-mutated lesions are clearly positive.[19] Decreased GS staining has been reported to occur in congested livers (including congestive heart failure and hepatic cirrhosis) and diseases that result in venous occlusion.[16] In our study, GS represented the single most-sensitive marker for identifying murine hepatocellular neoplasms. All tumors showed some positive staining of cells outside of zone 3 hepatocytes, and this distribution seems to be indicative of neoplastic transformation in the mouse liver. A less dramatic response has been reported in humans, in which GS stains 54% to 70% of HCC.[33,49] Positive staining for GS was consistently present in all HCC variants, adenomas, and FCA in the current study (Figure 4). Some clear-cell foci were located quite near zone 3 hepatocytes (Figure 4 B), causing us to wonder whether these foci are commonly zonal in location such that their GS staining positivity reflects their microanatomy. In addition, vacuolated foci stained positive, prompting the concern that they are preneoplastic lesions. Previously reported evidence suggests that FCA are preneoplastic lesions that can progress to neoplasia, given that these lesions can be induced by hepatocarcinogens and
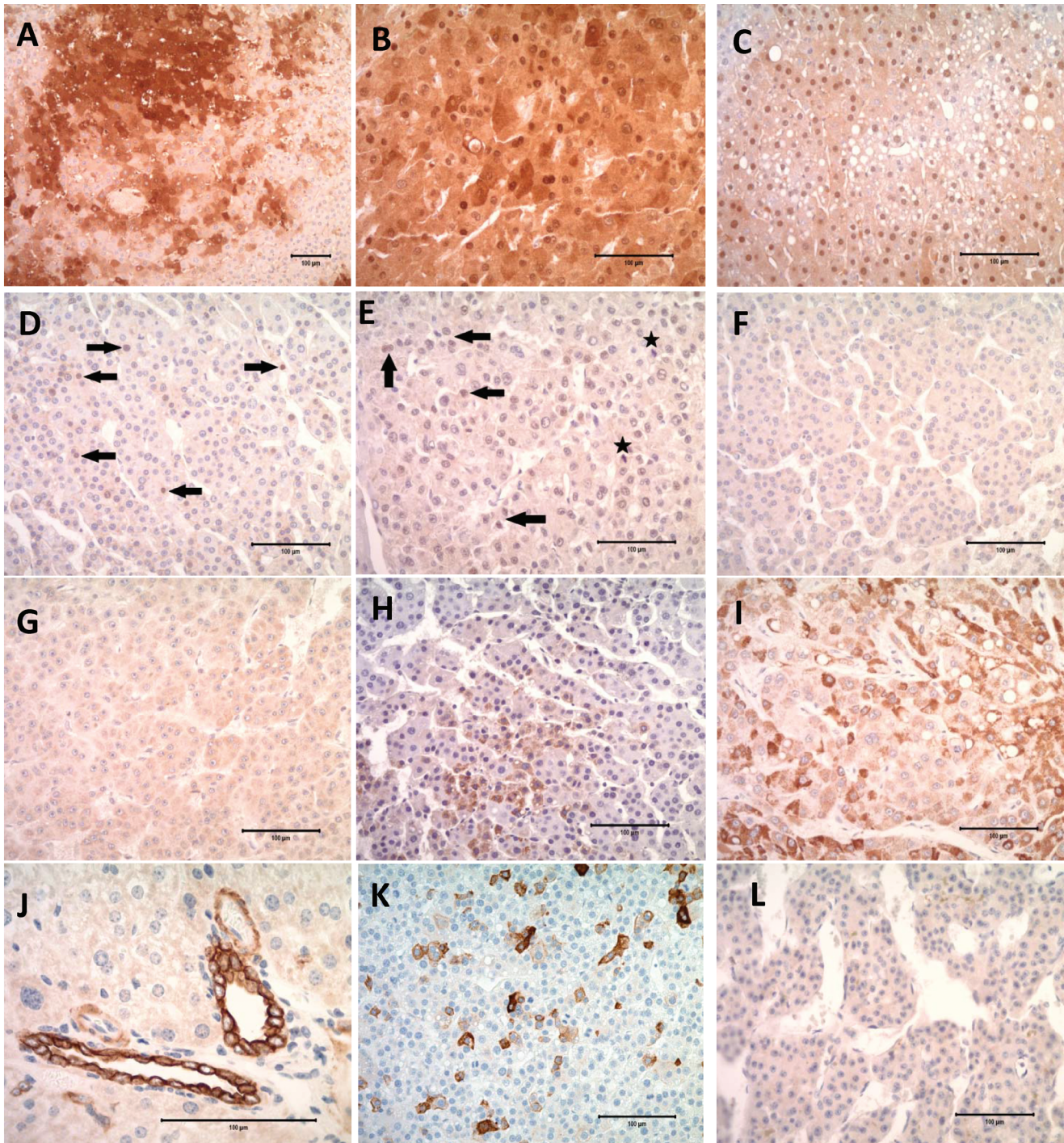
Figure 3. (A) Mouse Solid HCC showing Arg1-positive cytoplasmic and nuclear staining; magnification, 10×. (B) Human HCC showing Arg1-positive cytoplasmic and nuclear staining; magnification, 20×. (C) Mouse vacuolated foci showing some Arg1-positive nuclear staining of vacuolated hepato-cytes; magnification, 20×. (D) Mouse trabecular HCC showing nuclear staining of tumor cells with β-catenin (arrow); magnification, 20×. (E) Human HCC showing nuclear staining of tumor cells with β-catenin (arrow) and β-catenin-positive mitotic figures (star); magnification, 20×. (F) Glyp3-positive mouse Trabecular HCC showing light membranous staining; magnification, 20×. (G) Glyp3-positive human HCC showing light cytoplasmic and membranous staining; magnification, 20×. (H) Mouse trabecular HCC showing cytoplasmic staining for HepPar1; magnification, 20×. (I) Human HCC showing cytoplasmic staining for HepPar1; magnification, 20×. (J) Normal mouse liver showing typical intense staining of cholangiolar cells with CK19; magnification, 40×. (K) Mouse trabecular HCC showing intense cytoplasmic staining of scattered tumor cells with CK19; magnification, 20×. (L) CK19-negative human HCC; magnification, 20×.
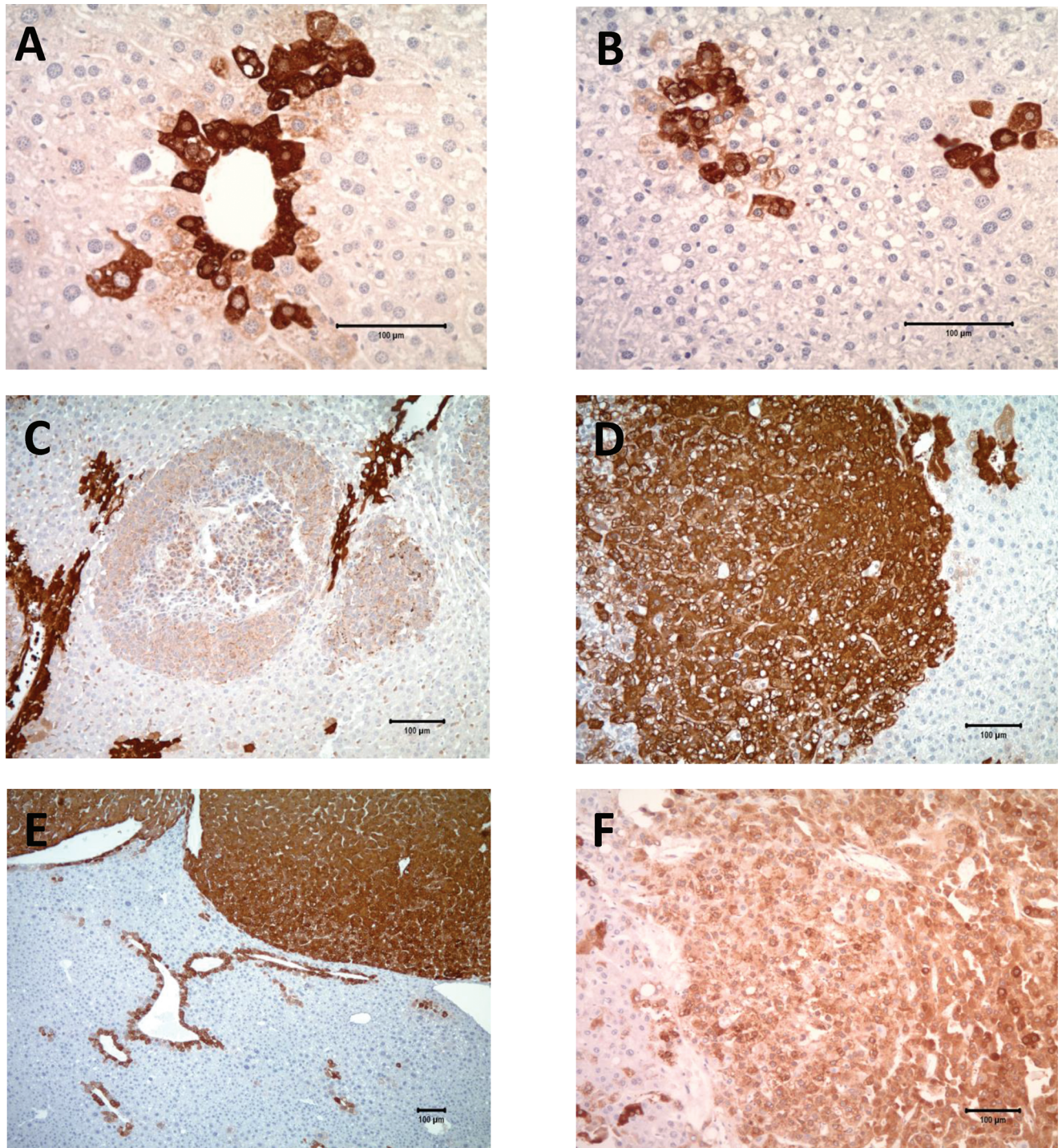
Figure 4. Glutamine synthetase (GS) immunohistochemistry, with most sections showing cytoplasmic and membranous staining of varying intensity. (A) Normal liver (mouse): intense GS staining of zone 3 hepatocytes; magnification, 20×. (B) Clear-cell focus (mouse) showing intense GS staining of zone 3 hepatocytes that are incorporated into the focus; magnification, 20×. (C) Adenoid HCC (mouse) showing intense GS staining of zone 3 hepatocytes, with lighter-staining tumor cells; magnification, 10×. (D) Solid HCC (mouse) with positive GS staining of tumor cells; magnification, 10×. (E) Trabecular HCC (mouse) with intense GS staining of tumor cells that are well-outlined and -circumscribed. Normal perivenular staining is present as well; magnification, 5×. (F) Human HCC showing moderate cytoplasmic and membranous GS staining of neoplastic cells; magnification, 10×.

that hepatocytes within the various foci have a phenotype distinct from adjacent hepatocytes.[36] Furthermore, there is an association between FCA and their progression to adenomas and carcinomas in carcinogen-induced hepatocellular tumors.[7] Given the sensitivity of GS staining and the ability to use it for quick evaluation of mouse tumors by gross visualization of the slide, this immunomarker represents a valuable component of a diagnostic immunohistochemical staining panel.

The Glyp3 antigen is present in human HCC, with less sensitivity in well-differentiated HCC compared with poorly differentiated HCC and no staining noted in adenomas.[47,59] Human HCC that develop in areas of hepatic cirrhosis are more often positive for Glyp3 than are those not within cirrhotic foci.[47] Murine FCA and tumors in the current study showed faint staining, with minimal differences noted between adenomas and the HCC variants, except for solid HCC. Consequently, the staining trends for Glyp3 are difficult to interpret in the mouse models we used.

HepPar1 staining of murine FCA and tumors was extremely variable (23% to 73%), whereas all of the human HCC were positive, thus exceeding the reports of 26% to 70% positivity.[29,42] The few human HCC samples (*n* = 5) used for our study may be a factor in this staining prevalence. HepPar1 normally is found in normal and neoplastic hepatocytes, and we expected the staining results to be positive in more of the mouse FCA and tumor types than was demonstrated. More murine trabecular HCC expressed HepPar1 than did any other FCA or tumor type. HepPar1 is included in human immunohistochemistry panels to distinguish tumors of hepatic origin from metastatic carcinomas, and HepPar1 has been reported to stain as many as 92% of human HCC.[4,8,17,41] Expression decreases in higher grade human tumors, with well-differentiated HCC showing 100% reactivity and high-grade carcinomas dropping to 83%. Human HCC with solid or sarcomatoid growth patterns are less likely to show immunoreactivity to HepPar1 than are other subtypes of HCC.[8] Other neoplasms that can stain positively for HepPar1 include adenocarcinomas of gastric, esophageal, ovarian, and pulmonary origins.[4,8,41]

CK19 is expressed in 10% to 100% of human cholangiocarcinoma and only 10% to 27% of human HCC;[2,13,27,31] We added CK19 to the immunopanel in an effort to differentiate these 2 tumors. In addition, CK19 provides some prognostic benefit, in that CK19-positive human HCC are larger, less differentiated, and show more vascular invasion correlating with a lower disease-free survival rate, than are CK19-negative HCC.[28,58] Furthermore, 28% of human HCC stained positively for either CK7 or CK19. The presence of CK19 in HCC might reflect a common progenitor cell:[13,52] CK19 is normally expressed in biliary epithelium in HCC and in trabecular hepatocytes of human HCC.[53] With only a small percentage (18%) of the mouse trabecular tumors showing scattered CK19-positive cells and with the absence of the acinar structures that are usually noted in cholangiocarcinoma, the likelihood of progenitor-cell CK19-positivity increases and the diagnosis of cholangiocarcinoma becomes less likely. For further confirmation of the effect of staining of progenitor cells, immunohistochemical staining of a group of mouse cholangiocarcinomas would be an interesting comparison with the data we present here.

Other markers that we considered adding to our panel include polyclonal carcinoembryonic antigen (pCEA), MOC31, and heat-shock protein 70 (HSP-70). pCEA is a glycoprotein of fetal epithelial cells that leads to staining of the cell membrane or cytoplasm in various adenocarcinomas; it also stains hepatic canaliculi. Intense canalicular staining can be misinterpreted as the cytoplasmic staining seen in adenocarcinomas, thus confounding interpretation. In addition, pCEA has low sensitivity in poorly differentiated HCC.[25,27,39,53] MOC31 is a cell-surface glycoprotein that typically is used to define human cholangiocarcinoma from HCC, but this antigen often shows weak immunostaining, decreasing its utility.[39,53] HSP70 has been proposed as a marker that is upregulated in HCC. However, its specificity is limited, in that

increased HSP70 intensity in immunohistochemically stained liver sections has been correlated with elevated serum levels of the protein in chronic hepatitis, cirrhosis, HCC, and metastatic relapse of HCC.[18,50] Furthermore, α-fetoprotein, an oncofetal protein that is specific for hepatocyte differentiation, has been used in the past to identify HCC but has a low sensitivity. Markers more sensitive than α-fetoprotein have now been identified, thus reducing the benefits of its use.[31]

Although not determined at the time of the initial experiment, the mouse colony was presumed to be positive for *Helicobacter* spp. *Helicobacter* infection might have potentiated hepatic neoplasia in these mice, given that *Helicobacter hepaticus* infection commonly causes chronic inflammation of the liver and subsequent development of hepatocellular tumors.[55] Because the current study focused on defining the immunohistochemical staining trends of FCA and tumors in mouse models, the etiopathogenesis of the tumors may not be as important as are their staining characteristics. Similarly, development of FCA has been associated with *H. hepaticus* infection, but such samples typically have oval cell hyperplasia with or without pseudocholangiolar formation,[43] features that were absent from the current samples.

Limitations of our study include low numbers of mice and, due to its retrospective nature, preanalytical variables such as the use of paraformaldehyde as a fixative and changing from the use of paraformaldehyde to alcohol for the mouse tissues, a modification that might have resulted in lower-than-expected positivity rates for some of the antibodies, such as Arg1 and HepPar1

In conclusion, we noted several trends in the immunostaining results from various mouse FCA and adenomas and mouse and human HCC. Antibodies commonly used in medical practice for the diagnosis of human HCC may be useful in mouse models to characterize the spectrum of primary liver tumor progression and to help distinguish primary liver tumors from metastasis models in models of neoplasia that may spread to the liver. The antibodies we chose to assess have similar performance characteristics—and limitations—in mouse compared with human tissue. Consistently performing a full immunopanel comprising Arg1, β-catenin, CK19, GS, Gyp3, and HepPar1 is probably cost-prohibitive and unnecessary, given the current study results that GS positivity outside of zone 3 seems to indicate hepatocellular alteration. More investigation is still needed with mouse models of hepatic neoplasia, but the use of GS appears to be most valuable in identifying neoplasia in the transgenic mouse models we tested and should be included in immunohistochemistry assessing hepatocellular neoplasia development.

References

1. **Balaton AJ, Nehama-Sibony M, Gotheil C, Callard P, Baviera EE.** 1988. Distinction between hepatocellular carcinoma, cholangiocarcinoma, and metastatic carcinoma based upon immunohistochemical staining for carcinoembryonic antigen and cytokeratin 19 on paraffin sections. J Pathol **156:**305–310.
2. **Behrens J, Lustig B.** 2004. The Wnt connection to tumorigenesis. Int J Dev Biol **48:**477–487.
3. **Blanc JF, Frulio N, Chiche L, Sempoux C, Annet L, Hubert C, Gouw ASH, deJong KP, Bioulac-Sage P, Blabaud C.** 2015. Hepatocellular adenoma management: call for shared guidelines and multidisciplinary approach. Clin Res Hepatol Gastroenterol **39:**180–187.

4. **Butler SL, Dong H, Cardona D, Jia M, Zheng R, Zhu H, Crawford JM,** Liu C. 2007. The antigen for HepPar1 antibody is the urea cycle enzyme carbamoyl phosphate synthetase 1. Lab Invest **88:**78–88.

5. **Caldwell S, Park SH.** 2009. The epidemiology of hepatocellular cancer: from the perspectives of public health problem to tumor biology. J Gastroenterol **44** (Suppl 19)**:**96–101.

6. **Calvisi DF, Factor VM, Loi R,** Thorgeirsson SS. 2001. Activation of β-catenin during hepatocarcinogenesis in transgenic mouse models: relationship to phenotype and tumor grade. Cancer Res **61:**2085–2091.

7. **Carter JH, Carter HW, Deddens JA, Hurst BM, George MH, DeAngelo AB**. 2003. A 2-year dose response study of lesion sequences during hepatocellular carcinogenesis in the male B6C3F1 mouse given the drinking water chemical dichloroacetic acid. Environ Health Perspect **111:**53–64.

8. **Chu PG, Ishizawa S, Wu E, Weiss LM.** 2002. Heptaocyte antigen as a marker of hepatocellular carcinoma. Am J Surg Pathol **26:**978–988.

9. **Clinkenbeard EL, Butler JE, Spear BT.** 2012. Pericentral activity of α-fetoprotein enhancer 3 and glutamine synthetase upstream enhancer in the adult liver are regulated by β-catenin in mice. Hepatology **56:**1892–1901.

10. **Deane NG, Lee H, Hamaamen J, Ruley A, Washington MK, LaFleur B, Thorgeirsson SS, Price R, Beauchamp RD.** 2004. Enhanced tumor formation in cyclin D1 × transforming growth factor β1 double-transgenic mice with characterization by magnetic resonance imaging. Cancer Res **64:**1315–1322.

11. **Deane NG, Parker MA, Aramandla R, Diehl L, Lee W-J, Washington MK, Nanney LB, Shyr Y, Beauchamp RD.** 2001. Hepatocellular carcinoma results from chronic cyclin D1 overexpression in transgenic mice. Cancer Res **61:**5389–5395.

12. **Deschl U, Cattley RC, Harada T, Kuttler K, Hailey JR, Hartig F, Leblanc B, Marsman DS, Shirai T.** 2001. Liver, gallbladder and exocrine pancreas, p 60–68. In: Mohr U, editor. International classification of rodent tumors—the mouse. New York (NY): Springer–Verlag.

13. **Durnez A, Verslype C, Nevens F, Fevery J, Aerts R, Pirenne J, Lesaffre E, Libbrecht L, Desment V, Roskams T.** 2006. The clinicopathological and prognostic relevance of cytokeratin 7 and 19 expression in hepatocellular carcinoma. A possible progenitor-cell origin. Histopathology **49:**138–151.

14. **El-Serag HB.** 2007. Epidemiology of hepatocellular carcinoma in USA. Hepatol Res **37** (Suppl 2)**:**S88–S94.

15. **Fatima N, Cohen C, Siddiqui MT.** 2014. Arginase 1: a highly specific marker separating pancreatic adenocarcinoma from hepatocellular carcinoma. Acta Cytol **58:**83–88.

16. **Fleming KE, Wanless IR.** 2013. Glutamine synthetase expression in activated hepatocyte progenitor cells and loss of hepatocellular expression in congestion and cirrhosis. Liver Int **33:**525–534.

17. **Fujiwara M, Kwok S, Yano H, Pai RK.** 2012. Arginase 1 is a more sensitive marker of hepatic differentiation than HepPar1 and glypican 3 in fine-needle aspiration biopsies. Cancer Cytopathol **120:**230–237.

18. **Gehrmann M, Cervello M, Montalto G, Cappello F, Gulino A, Knape C, Specht HM, Multhoff G.** 2014. Heat-shock protein 70 serum levels differ significantly in patients with chronic hepatitis, liver cirrhosis, and hepatocellular carcinoma. Front Immunol **5:**307.

19. **Hailfinger S, Jaworski M,** Braeuning A, Buchmann A, Schwarz M. 2006. Zonal gene expression in murine liver: lessons from tumors. Hepatology **43:**407–414.

20. **Herzer K, Carbow A, Sydor S, Sowa JP, Biesterfeld S, Hofmann TG, Galle PR, Gerken G, Canbay A.** 2012. Deficiency of the promyleocytic leukemia protein fosters hepatitis C-associated hepatocarcinogenesis in mice. PLoS One **7:**e44474.

21. **Hsu HC, Jeng YM, Mao TL, Chu JS, Lai PL, Peng SY.** 2000. β-catenin mutations are associated with a subset of low-stage hepatocellular carcinoma negative for hepatitis B virus and with favorable prognosis. Am J Pathol **157:**763–770.

22. **Ishak KG, Goodman ZD, Stocker JT.** 2001. Tumors of the liver and intrahepatic bile ducts: atlas of tumor pathology, 3rd series, fascicle 31. Washington (DC): Armed Forces Institute of Pathology.

23. **Jang JJ, Weghorst CM, Henneman JR, Devor DE, Ward JM.** 1992. Progressive atypia in spontaneous and N-nitrosodiethylamine-induced hepatocellular adenomas of C3H/HeNCr mice. Carcinogenesis **13:**1541–1547.

24. **Jemal A, Bray F, Center MM, Ferlay J, Ward E, Forman D.** 2011. Global cancer statistics. CA Cancer J Clin **61:**69–90.

25. **Kakar S, Gown AM, Goodman ZD, Ferrell LD.** 2007. Best practices in diagnostic immunohistochemistry hepatocellular carcinoma versus metastatic neoplasms. Arch Pathol Lab Med. **131:**1648–1654.

26. **Kandil DH, Cooper K.** 2009. Glypican 3: a novel diagnostic marker for hepatocellular carcinoma and more. Adv Anat Pathol **16:**125–129.

27. **Karabork A, Kaygusuz G, Ekinci C.** 2010. The best immunohistochemical panel for differentiating hepatocellular carcinoma from metastatic adenocarcinoma. Pathol Res Pract **206:**572–577.

28. **Kim H, Choi GH, Na DC, Ahn EY, Kim GI, Lee JE, Cho JY, Yoo JE, Choi JS, Park YN.** 2011. Human hepatocellular carcinomas with 'stemness'-related marker expression: keratin 19 expression and a poor prognosis. Hepatology **54:**1707–1717.

29. **Krings G, Ramachandran R, Jain D, Wu TT, Yeh MM, Torbenson M, Kakar S.** 2013. Immunohistochemical pitfalls and the importance of glypican 3 and arginase in the diagnosis of scirrhous hepatocellular carcinoma. Mod Pathol **26:**782–791.

30. **Lahousse SA, Hoenerhoff M, Collins J, Ton T-VT, Masinde T, Olson D, Rebolloso Y, Koujitani T, Tomer KB, Hong H-HL, Bucher J, Sills RC.** 2010. Gene expression and mutation assessment provide clues of genetic and epigenetc mechanisms in liver tumors of oxazepam-exposed mice. Vet Pathol **48:**875.

31. **Lau SK, Prakash S, Geller SA, Alsabeh R.** 2002. Comparative immunohistochemical profile of hepatocellular carcinoma, cholangiocarcinoma, and metastatic adenocardinoma. Hum Pathol **33:**1175–1181.

32. **Lee JI, Lee JW, Kim JM, Kim JK, Chung HJ, Kim YS.** 2012. Prognosis of hepatocellular carcinoma expressing cytokeratin 19: comparison with other liver cancers. World J Gastroenterol **18:**4751–4757.

33. **Long J, Lang ZW, Wang HG, Wang TL, Wang BE, Liu SQ.** 2010. Glutamine synthetase as an early marker for hepatocellular carcinoma based on proteomic analysis of resected small hepatocellular carcinomas. Hepatobiliary Pancreat Dis Int **9:**296–305.

34. **Mahon DC.** 1989. Altered hepatic foci in rat liver as weight of evidence of carcinogenicity: the Canadian perspective. Toxicol Pathol **17:**709–715.

35. **Maranpot RR, Boorman GA, Gaul BW, editors.** 1999. Pathology of the mouse: reference and atlas, p 146–149. St Louis (MO): Cache River Press.

36. **Maronpot RR, Harada T, Murthy AS, Boorman GA.** 1989. Documenting foci of hepatocellular alteration in two-year carcinogenicity studies: current practices of the National Toxicology Program. Toxicol Pathol **17:**675–683.

37. **Maeda T, Kajiyama K, Adachi E**, **Takenaka K, Sugimachi K, Tsuneyoshi M.** 1996. The expression of cytokeratins 7, 19, and 20 in primary and metastatic carcinomas of the liver. Mod Pathol **9:**901–909.

38. **McKnight R, Nassar A, Cohen C, Siddiqui MT.** 2012. Arginase 1: a novel immunohistochemical marker of hepatocellular differentiation in fine needle aspiration cytology. Cancer Cytopathol **120:**223–229.

39. **Morrison C, Marsh W Jr, Franke WL.** 2002. A comparison of CD10 to pCEA, MOC31, and hepatocyte for the distinction of malignant tumors in the liver. Mod Pathol **15:**1279–1287.

40. **National Institutes of Health.** [Internet]. 2013. Estimates of funding for various research, condition, and disease categories (RCDC). Research Portfolio Online Reporting Tools (RePort). [Cited 24 Feb 2014]. Available at: http://report.nih.gov/PFSummaryTable.aspx

41. **Pang Y, von Turkovich M, Wu H, Mitchell J.** Mount S, Taatjes D, Cooper K. 2006. The binding of thyroid transcription factor 1 and hepatocyte paraffin 1 to mitochondrial proteins in hepatocytes: a molecular and immunoelectron microscopic study. Am J Clin Pathol **125:**722–726.

42. **Radwan NA, Ahmed NS.** 2012. The diagnostic value of arginase-1 immunostaining in differentiating hepatocellular carcinoma from

metastatic carcinoma and cholangiocarcinoma as compared to Hep-Par1. Diagn Pathol **7:**149.

43. **Rogers AB, Boutin SR, Whary MT, Sundina N, Ge Z, Cormier K, Fox JG.** 2004. Progression of chronic hepatitis-infected A/JCr mice. Toxicol Pathol **32:**668–677.

44. **Ryu HS, Lee K, Shin E, Kim SH, Jing J, Jung HY, Lee H, Jang JJ.** 2012. Comparative analysis of immunohistochemical markers for differential diagnosis of hepatocellular carcinoma and cholangiocarcinoma. Tumori **98:**478–484.

45. **Sanderson N, Factor V, Nagy P, Kopp J, Kondaiah P, Wakefield L, Roberts AB, Sporn MB, Thorgeirsson SS.** 1995. Hepatic expression of mature transforming growth factor β1 in transgenic mice results in multiple tissue lesions. Proc Natl Acad Sci USA **92:**2572–2576.

46. **Siegel R, Naishadham D, Jemal A.** 2013. Cancer statistics 2013. CA Cancer J Clin **63:**11–30.

47. **Shafizadah N, Ferrell LD, Kakar S.** 2008. Utility and limitations of glypican-3 expression for the diagnosis of hepatocellular carcinoma at both ends of the differentiation spectrum. Mod Pathol **21:**1011–1018.

48. **Shafizadeh N, Kakar S.** 2011. Diagnosis of well-differentiated hepatocellular lesions: role of immunohistochemistry and other ancillary techniques. Adv Anat Pathol **18:**438–445.

49. **Shin E, Ryu HS, Kim SH, Jung H, Jang JJ, Lee K.** 2011. The clinicopathological significance of heat shock protein 70 and glutamine synthetase expression in hepatocellular carcinoma. J Hepatobiliary Pancreat Sci **18:**544–550.

50. **Tan GS, Lim KH, Tan HT, Khoo ML, Tan SH, Toh HC, Chung MCM.** 2014. Novel proteomic biomarker panel for prediction of aggressive metastatic hepatocellular carcinoma relapse in surgically resectable patients. J Proteome Res **13:**4833–4846.

51. **Thoolen B, Maronpot RR, Harada T, Nyska A, Rousseaux C, Nolte T, Malarkey DE, Kaufmann W, Kuttler K, Deschl U, Nakae D, Gregson R, Vinlove MP, Brix AE, Singh B, Belpoggi F, Ward JW.** 2010. Proliferative and nonproliferative lesions of the rat and mouse hepatobiliary system. Toxicol Pathol **38**(7 Suppl)**:**5S–81S.

52. **Timek DT, Shi J, Liu H, Lin F.** 2012. Arginase 1, HepPar1, and glypican 3 are the most effective panel of markers in distinguishing hepatocellular carcinoma from metastatic tumor on fine-needle aspiration specimens. Am J Clin Pathol **138:**203–210.

53. **Tsuji M, Kashihara T, Terada N, Mori H.** 1999. An immunohistochemical study of hepatic atypical adenomatous hyperplasia, hepatocellular carcinoma, and cholangiocarcinoma with α-fetoprotein, carcinoembryonic antigen, CA19-9, epithelial membrane antigen, and cytokeratins 18 and 19. Pathol Int **49:**310–317.

54. **Van Nhieu JT, Renard CA, Wei Y, Cherqui D, Zafrani ES, Buendia MA.** 1999. Nuclear accumulation of mutated β-catenin in hepatocellular carcinoma is associated with increased cell proliferation. Am J Pathol **155:**703–710.

55. **Ward JM, Fox JG, Anver MR, Haines DC, George CV, Collins MJ Jr, Gorelick PL, Nagashima K, Gonda MA, Gilden RV, Tully JG, Russell RJ, Benveniste RE, Paster BJ, Dewhirst FE, Donovan JC, Anderson LM, Rice JM.** 1994. Chronic active hepatitis and associated liver tumors in mice caused by a persistent bacterial infection with a novel *Helicobacter* species. J Natl Cancer Inst **86:**1222–1227.

56. **Wennerberg AE, Nalesnik MA, Coleman WB.** 1993. Hepatocyte paraffin 1: a monoclonal antibody that reacts with hepatocytes and can be used for differential diagnosis of hepatic tumors. Am J Pathol **143:**1050–1054.

57. **Wu PC, Fang JW, Lau VK, Lai CL, Lo CK, Lau JY.** 1996. Classification of hepatocellular carcinoma according to hepatocellular and biliary differentiation markers. Am J Pathol **149:**1167–1175.

58. **Witjes CD, ten Kate FJ, Verhoef C, de Man RA, IJzermans JN.** 2013. Immunohistochemical characteristics of hepatocellular carcinoma in noncirrhotic livers. J Clin Pathol **66:**687–691.

59. **Yamauchi N, Watanabe A, Hishinuma M, Ohashi K, Midorikawa Y, Morishita Y, Niki T, Shibahara J, Mori M, Makuuchi M, Hippo Y, Kodama T, Iwanari H, Aburatani H, Fukayama M.** 2005. The glypican 3 oncofetal protein is a promising diagnostic marker for hepatocellular carcinoma. Mod Pathol **18:**1591–1598.

60. **Yan BC, Gong C, Song J, Krausz T, Tretiakova M, Hyjek E, Al-Ahmadie H, Alves V, Xiao SY, Anders RA, Hart JA.** 2010. Arginase 1: a new immunohistochemical marker of hepatocytes and hepatocellular neoplasms. Am J Surg Pathol **34:**1147–1154.

61. **Zhu ZW, Friess H, Wang L, Abou-Shady M, Zimmermann A, Lander AD, Korc M, Kleeff J, Buchler MW.** 2001. Enhanced glypican-3 expression differentiates the majority of hepatocellular carcinomas from benign hepatic disorders. Gut **48:**558–564.